

# A Tabletop Mid-Infrared Nulling Testbed for the Keck Interferometer and the Terrestrial Planet Finder

Chris Koresko<sup>a</sup>, Bertrand Mennesson<sup>b</sup>, Samuel Crawford<sup>b</sup>,  
Michelle Creech-Eakman<sup>b</sup>, Kent Wallace<sup>b</sup>, Eugene Serabyn<sup>b</sup>

<sup>a</sup>Interferometry Science Center, Caltech, Pasadena, CA, USA

<sup>b</sup>Jet Propulsion Laboratory, Caltech, Pasadena, CA, USA

## ABSTRACT

A rotational-shearing tabletop interferometer experiment has been constructed and operated at JPL to serve as a testbed for the mid-infrared ( $\sim 10 \mu\text{m}$ ) nulling beam combiners on the Keck Interferometer and the Terrestrial Planet Finder. The testbed is a pupil-plane combiner in which destructive combination of the incoming wavefronts is achieved using a rooftop mirror system in which the polarization vector is flipped along the vertical axis on one arm and the horizontal axis on the other. The optical pathlength along one arm is adjustable using a linear stage driven by picomotor and piezoelectric actuators. The combined light is focussed onto a single-pixel  $\text{LN}_2$ -cooled HgCdTe detector. In order to provide adequate sensitivity in the presence of the very bright thermal emission from the room-temperature optics, the light source is modulated and the output is demodulated using a lock-in amplifier. The optical pathlength difference (OPD) is stabilized under computer control by dithering the actuated arm and balancing the leakage signal on either side of the null. The system has produced a stabilized null depth of  $6 \times 10^{-5}$  using a diode laser source at a wavelength of  $9 \mu\text{m}$ , and unstabilized nulls of  $< 3 \times 10^{-3}$  with a broadband thermal IR source. The latter measurement was limited by the noise floor of the detector.

**Keywords:** Interferometry, Field-Flip, Astronomy, Infrared, Laboratory

## 1. INTRODUCTION

The introduction of a 180-degree relative rotational shear, or “field flip”, into the inputs of a pupil-plane beam combiner is currently the favored approach for producing deep achromatic nulls for the mid-infrared version of the Terrestrial Planet Finder (TPF) mission. A deep null centered on a bright star would permit detection and spectroscopy of the  $\sim 10^6$  times fainter light coming from an Earthlike planet at an angular distance of only  $\sim 0''.1$  from the star.

In order to explore the use of a “field-flip” nulling beam combiner (“nuller”) operating at mid-infrared wavelengths, we have constructed and operated a tabletop demonstrator at JPL. The basic design of the instrument is very similar to that which has previously been used successfully at visible wavelengths (Serabyn 1999). The fundamental idea is straightforward. In brief, the field flip is produced by adding to a typical Michelson-style interferometer a pair of rooftop mirrors, one placed in each of the arms, and oriented such that the peak of one rooftop (the “spine”) is perpendicular to that of the other. Reflection by each rooftop reverses the sign of the vector component of the electric field which lies perpendicular to the spine. As a result, the beam combination occurs after the field in one arm has been flipped in the horizontal axis while the field in the other arm has been flipped in the vertical axis, so that for zero optical pathlength difference (OPD) the overall electric field vectors are opposed at the point of combination. This should in principle produce an achromatic null fringe. An additional flat mirror is inserted into each arm in order to balance the total number of s-plane and p-plane reflections. A schematic of the optical path is shown in Figure 1.

This instrument has reached null depths, defined as the ratio of the output intensity at the destructive fringe to that at the constructive fringe, of  $6 \times 10^{-5}$  using a diode laser source at a wavelength of  $9 \mu\text{m}$ , and sustained them using a simple pathlength-dithering servo system. Unstabilized nulls of  $< 3 \times 10^{-3}$  have also been produced with a broadband thermal infrared source. This paper describes the instrument and offers some general conclusions about the usefulness of this rooftop field-flip approach for nulling in the thermal infrared.

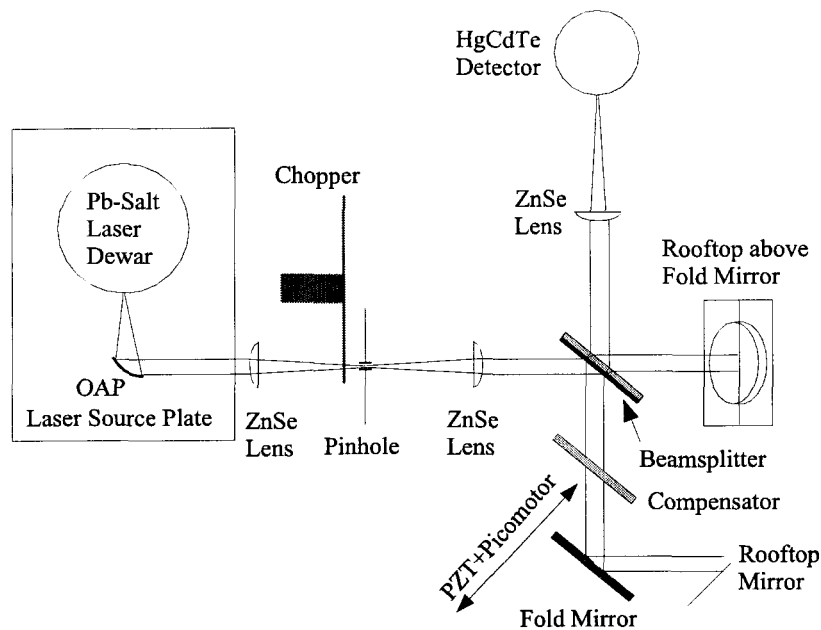


**Figure 1.** Tabletop nuller optical system configured with the diode laser as a light source. The system is conceptually very similar to the visible-light nuller described in Serabyn et al. (1999). The light is roughly collimated by an off-axis paraboloid, modulated by a rotating chopper wheel, and focussed onto a pinhole which acts as a spatial filter. The filtered light is then recollimated and split, with approximately half of the photons sent to each of the two arms. Each arm reverses one vector component of the polarization, so that when the beams are recombined at the beamsplitter, the interference is achromatically destructive when the OPD is zero. The pathlength in one arm can be adjusted by moving its fold mirror in the direction shown, under control of either a picomotor or a PZT actuator.

Because the instrument described here is closely related to the visible-light rooftop nuller, the emphasis will be on those aspects which are unique to operation at the longer wavelengths.

## 2. OPTICAL SYSTEM

The optical design of the apparatus described in this paper is conceptually a straightforward adaptation of the design described in Serabyn et al. (1999). Changes relative to the previous design were driven mainly by the requirement to produce, transmit, and detect light at thermal infrared rather than visible wavelengths. The optical changes involved the use of a pinhole rather than a single-mode fiber for spatially filtering the input light source (since no adequate single-mode fibers usable at  $10\ \mu\text{m}$  were available), bare gold reflecting surfaces (for high throughput and weak polarization effects), and ZnSe transmitting optics (lenses, the beamsplitter substrate, and its compensator).

The basic layout of the optical system is shown in Figure 1. As shown, the system is set up to use a mid-infrared diode laser as a light source, and to modulate it using a chopper wheel. Experiments were done with several additional configurations. These differ from the one shown only in their input and output. For example, for certain tests a wire-grid linear polarizer was inserted in the collimated space between the source and the beamsplitter. For broadband testing, the laser source was sometimes replaced by a thermal emitter and collimating lens. A second spatial filter (pinhole and focusing lens) just ahead of the detector was sometimes installed. Various objects were placed in the arms to attenuate the brighter beam and thereby match the fluxes in the two arms. Throughout these tests, however, the heart of the system, consisting of the beamsplitter, compensator, fold mirrors, and rooftops, remained intact.

### 3. LIGHT SOURCES AND DETECTOR

Both a broadband unpolarized thermal emitter and a narrowband polarized laser source were used for the experiment. Although the thermal source more closely approximates the light from an astrophysical target such as a star, dust disk, or planet, several factors make it much more challenging to achieve a deep null with it. Chromatic dispersion due to unbalanced pathlengths through the various dispersive components in the system (including coatings and the substrates of transmissive optics) is expected to be a significant contributor to the leakage through the null. Vertically and horizontally polarized components of light suffer different phase delays as they pass through dielectric stacks which are not perpendicular to the propagation direction. Both of these effects, which cause the null fringe to be blurred because they make the fringe position dependent on the characteristics of the photons, are greatly alleviated when the light is narrowband and vertically polarized. In addition, it is not trivial to reach sufficient sensitivity to measure and track a deep null on a thermal source. This is because the interferometer has a very narrow field of view (limiting the product  $A\Omega$  of the emitting area and the solid angle into which photons emitted by it will be captured by the optical system) while the melting point of the emitting material limits the intensity of its emission.

The thermal source chosen for our experiment is essentially a tungsten-filament light bulb in which the usual glass envelope has been replaced by a metal can with a hermetically-sealed window. The window material is chosen to be transparent in the thermal infrared. We experimented with several window materials (ZnSe, antireflection-coated Ge, and  $\text{CaF}_2$ ) and found that the detected signal was weakest for the  $\text{CaF}_2$  unit and about equally strong for the other two. We chose to use the ZnSe unit because the window is transparent at visual wavelengths, making it convenient to see when the source was turned on and to visually estimate the temperature of the filament from its color. The nominal operating temperature of the filament is XXXXX. We found that it was possible to safely operate the unit with significantly more than its rated electrical current. However, because the thermal radiation occurs in the long-wavelength regime of the blackbody curve, the intensity is only linearly dependent on the filament temperature and overdriving the source provided only a modest boost in the detected signal.

The narrowband source used was a commercial lead-salt diode laser. This  $\text{LN}_2$ -cooled system produced a roughly-collimated continuous beam at a wavelength close to XXX  $\mu\text{m}$ , with a power of approximately XXX  $\mu\text{W}$ . Its output beam was partially vertically polarized. The beam was approximately collimated by an off-axis paraboloid mirror which was included with the unit.

The experiment requires a spatially-filtered, collimated source. This was produced by using a positive lens to make an image of the source on a pinhole, and a second positive lens one focal length further downstream to collimate the light. In practice, there is a tradeoff between the quality of the spatial filtering and the throughput, and several pinhole sizes were tried.

The detector used was a  $\text{LN}_2$ -cooled HgCdTe photodiode enclosed in a small dewar. The optical bandpass was limited by a filter behind the dewar window to XXX - XXX  $\mu\text{m}$ . Noise intrinsic to the detector, rather than the shot-noise statistics of the thermal infrared background, limited its sensitivity. The advantage of this detector is that it is small (the main body is about the size of a Coke can) inexpensive ( $\sim$  \$2500), and convenient to use (it reaches its cryogenic operating temperature within about 15 minutes of being filled). The detector is connected to a commercial preamplifier. In order to improve the sensitivity of the experiment, we have since obtained a new LHe-cooled single-pixel detector, but this was not operational at the time of the experiments described here.

The mid-infrared wavelength regime differs from the visible in that everything in a room-temperature lab, including the optical system itself, is a strong emitter, and the number of photons per second is generally much larger than unity. As a result, the noise in a measurement tends to be large, white, and independent of the signal. It is therefore very useful (to the point of being essentially necessary) to modulate the light source and synchronously demodulate the detected signal. This restricts the range of frequency and phase to which the system is sensitive to noise, and in typical conditions can greatly improve the overall sensitivity. This approach was implemented for our experiment.

Two source modulation schemes were tried. The first was to insert a mechanical chopper wheel close to the focus at the position of the spatial-filtering pinhole. This modulated the light from the emitter at a frequency

close to 800 Hz. The chopper controller provided TTL synchronization pulses with the same frequency as the modulation and at a constant phase relative to it. These pulses were fed to the reference input of a commercial lock-in amplifier.

The second scheme for modulating the infrared emission was used only for the laser source. The laser controller had an analog input which controlled the current to the laser. The lock-in amplifier was set to produce its own sine-wave reference signal, and this was connected to the laser controller's current control input. The modulation frequency could be varied over a wide range without much effect on the experiment.

The preamplified detector signal was connected to the signal input of the lock-in. Once the phase of the lock-in was adjusted correctly, the demodulated output became insensitive to essentially all unwanted photons, including the slowly-varying thermal background. This had the pleasant side effect of allowing the experiments to be run with the room lights on and the experimenters wandering around the instrument.

Unfortunately, both signal modulation schemes had significant drawbacks. There was some concern about the possibility that the air currents produced by a spinning chopper wheel could disturb the wavefront phases in the two arms of the interferometer, or that the mechanical vibrations associated with it could cause high-frequency modulation of the OPD. A more subtle problem arose due to the fact that the laser was kept at a temperature close to 80(?) K, well below the temperature of the chopper wheel. The rotation of the chopper wheel causes the detector to alternately see the cold laser or the warm blades of the wheel. This produces a signal whose phase is opposite that produced by the laser beam itself, effectively reducing the overall strength of the demodulated signal.

Modulating the laser emission via the drive current avoids this issue, but introduces another, potentially more serious one: the temperature of the laser substrate will vary, with a phase lag with respect to the emission. This will produce thermal emission with a similar phase lag. If the nuller is chromatic then the null will not be as deep for the thermal emission as for the laser emission, and the ratio of the narrowband intensity to the broadband intensity will be a function of the OPD. As a result, the phase of the modulated signal at the preamplifier will depend on the OPD. Depending on the details, this can produce an unknown bias in the demodulated signal which may be larger than the signal due to the leakage in the nulled laser emission. In experiments that followed the ones presented here, this possibility was partially addressed by conservatively choosing the "R" output of the lock-in, which measures the signal independent of the phase, rather than the phase-dependent "X" output. For future laser experiments, a better approach will likely be to install a narrowband optical filter before the detector.

#### 4. DATA SYSTEM AND SERVO

The lock-in amplifier used for this experiment was a rather sophisticated digital unit equipped with a standard RS-232 serial interface through which many amplifier parameters could be controlled and the output voltage read. In addition, the amplifier has a set of analog outputs which can be also controlled via the serial interface. One of these analog outputs was connected to the control input of the PZT actuator controller.

The amplifier was connected through this serial interface to a Linux-based personal computer. The computer's parallel port, which produces a set of TTL voltages controllable by writing to an I/O port address, was connected to the control input of the drive electronics box which controlled the picomotor actuator. The personal computer could therefore command motions of the OPD stage, set up the amplifier parameters, and read the amplitude of the resulting demodulated infrared signal.

A set of C programs was developed to control all of this, and to record the data to disk. The simplest experiments consisted of sweeping the OPD while periodically sampling the demodulated output signal. Short ( $\lesssim 100 \mu\text{m}$ ) sweeps could be made using the PZT, while longer sweeps (up to  $\sim 1 \text{ cm}$ ) required moving the picomotor. Each scan measured the fringe envelope, providing both an estimate of the nuller performance (*i.e.*, the null depth) and a qualitative estimate of the chromaticity of the fringe packet. Each picomotor step changed the OPD by a non-repeatable amount between  $\sim 20 - 30 \text{ nm}$ , depending on the position of the drive screw. This stepsize was small enough to sample nulls deeper than  $10^{-4}$ , and the null depth was found to be repeatable from one picomotor scan to the next.

Stabilization of the null was done by dithering the OPD using the PZT, *i.e.*, moving it by a small fraction of a wavelength first to one side of the current estimated null position and then to the other. If the signal in the three positions decreased monotonically in one direction, then the estimate of the null position (and the center of the dither pattern) was adjusted in that direction by a distance equal to the dither amplitude. Sets of samples taken at the estimated null position were averaged, and their average and RMS scatter were saved. This crude stabilization algorithm proved to converge relatively slowly to a nearby null (the upper limit on its speed was set by the product of the dither amplitude and dither frequency), but it was also rather robust. A more sophisticated approach based on fitting a parabola to the signals at the three dither points turned out to be unstable, for reasons which are not well understood.

## 5. EXPERIMENTAL RESULTS

A variety of experiments were conducted with the tabletop nuller, starting with simple scans through the fringe envelope and later progressing to increasingly deep stabilized nulls. This section presents a selection of the more interesting data they produced.

### 5.1. Scans through Fringe Packets in Broadband and Narrowband Light

Single scans were made stepping the OPD using the picomotor to move the fold mirror on one interferometer arm, and periodically sampling the demodulated signal from the lock-in amplifier. The scans were typically several hundred microns long, which was sufficient to cover the central fringe packet when a broadband source was used.

Here we present scans representing the extremes of the bandpasses we experimented with. The first scan was made using a thermal light source whose bandpass was limited by a  $\sim 30\%$  filter mounted inside the detector dewar. It is shown in Figure 2. The envelope is narrow, as expected, and the maximum intensity contrast is only 22. In addition, a closer examination of the scan reveals that it is significantly asymmetrical: Rather than the hoped-for deep central null surrounded by a pair of similar side-nulls, this scan shows a pair of adjacent nulls of similar depth and a central constructive peak. In addition, the sidelobes are quite unlike each other in detail. These characteristics point to uncorrected longitudinal dispersion in the system. In principle, this could have been corrected by adjusting the angle of the compensator plate, but that adjustment had not been done at the time this scan was made.

The second scan was made using the diode laser at a wavelength of  $9\ \mu\text{m}$ . It is plotted in Figure 3 with a logarithmic vertical scale to make the differences in the depths of the nulls visible. The narrow bandpass made the experiment relatively insensitive to residual chromatic dispersion, but there is still a noticeable asymmetry in the envelope. Despite this, the maximum fringe contrast is in excess of  $10^4$ .

### 5.2. Null Stabilization Results

Producing a stabilized null was an important goal for the tabletop infrared nuller experiment. As described in Section 4, it was accomplished in a simple way by comparing the demodulated signals as the OPD was dithered by a small fraction of a wavelength. Whenever the signal decreased monotonically in one direction during a dither pattern, the pattern was recentered on a position offset from the old one in that direction by one dither amplitude distance. The dither frequency was only a few Hertz, which was much less than the modulation frequency of the input light. Only the signal at the estimated position of the null was recorded. The stabilization system was used only with the laser, as the brightness of the thermal source was not adequate to allow deep nulls to be measured.

The result of a demonstration run of the stabilization system are plotted in Figure 4. The OPD was first tuned manually to a position close to a constructive fringe, and about 20 samples were recorded to establish a baseline. Then the OPD was manually tuned toward the position of the null, so that the demodulated signal intensity was reduced by a factor of about 10. At that point the system was left to seek the null, which it proceeded to do. Once the null position was reached, the system held it stably for some 200 sample periods until the OPD was again manually tuned to the constructive fringe. Note that the null stabilization servo was active throughout the experiment, but was ineffectual when the OPD was not set close to a null.

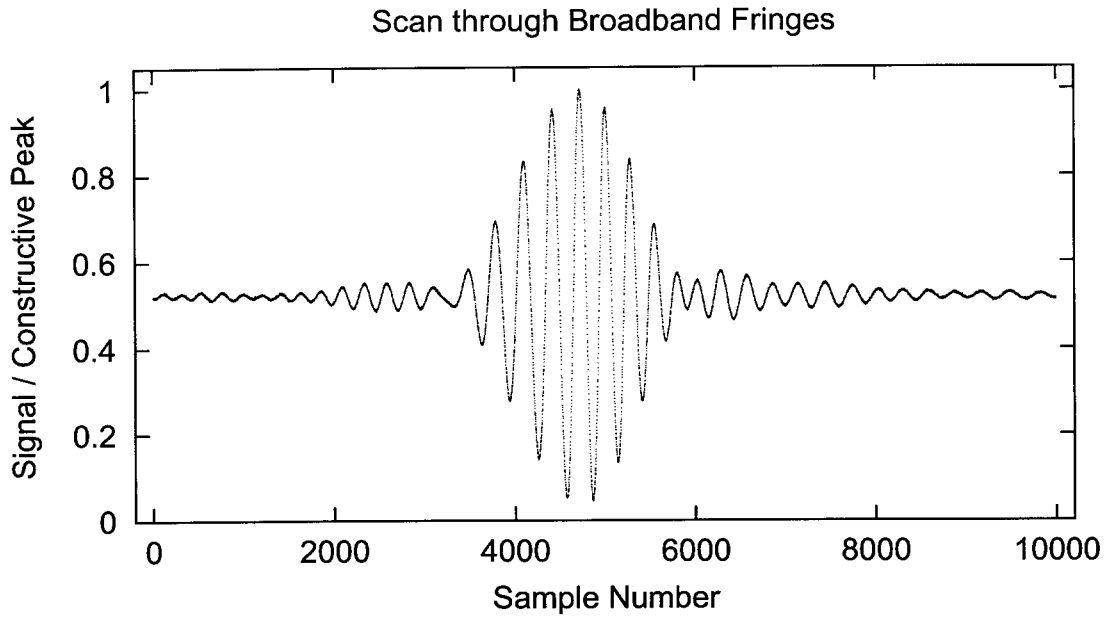


**Figure 2.** Scan through thermal emitter fringes with the optical bandpass defined by a  $\sim 30\%$  interference filter.

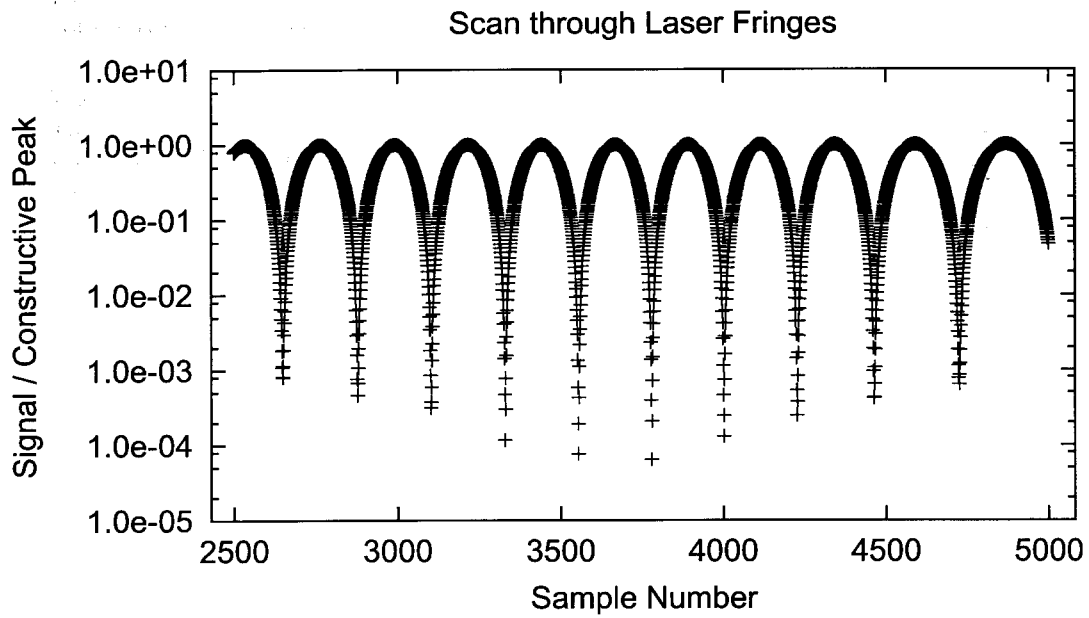


**Figure 3.** Scan through laser-light fringes with  $9 \mu\text{m}$  wavelength. Note the logarithmic vertical scale.

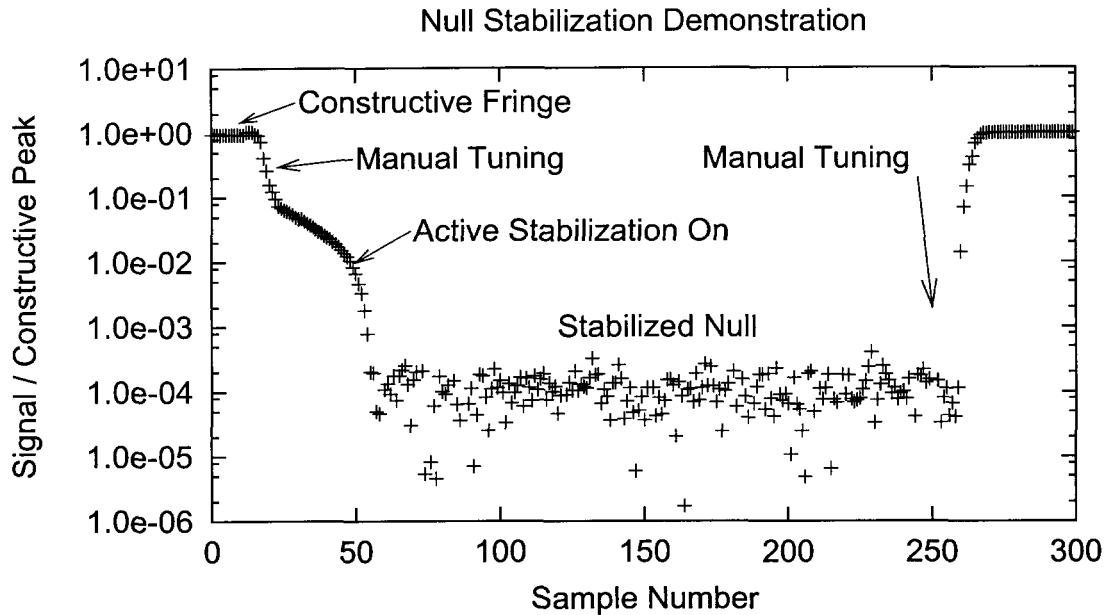


Figure 4. Demonstration of the stabilization of a laser-light null.

A second experiment was run after some refinements were made to the optics. In particular, a polarizer in the collimated space between the laser and the beamsplitter was carefully adjusted to optimize the null depth (see Section 5.3 for details). The system was then manually tuned close to the null and allowed to seek the best OPD under servo control. Groups of samples at the null position were averaged to improve the effective sensitivity and to provide noise estimates. The results, plotted in Figure 5, show the deepest stabilized null achieved with the rooftop nuller, with the nulled signal averaging only  $6 \times 10^{-5}$  of the constructive peak.

### 5.3. Sensitivity to Polarization of the Input Beam

The availability of the active stabilization system helped make it practical to explore the instrument's sensitivity to the polarization of the input light. It was feared that the presence of dielectric coatings (including several antireflection and beamsplitter coatings seen by the light in each path from the input of the system to the output) would cause unequal relative delays in the wavefront phases of horizontally and vertically polarized light. This led us to suspect that deeper nulls could be produced using a light source which was purely vertically polarized rather than in a mixed state.

This effect was searched for by inserting a wire-grid linear polarizer (on a ZnSe substrate) in the collimated space upstream of the beamsplitter. The polarizer mount permitted calibrated rotations, but the absolute orientation was not precisely known. The test consisted of locking the system on a null and monitoring the demodulated signal as the polarizer was set to a series of indicated position angles. This produced a smooth curve which was well fit by a quadratic close to its minimum (Figure 6), demonstrating both the polarization dependence and the effectiveness of the null stabilization servo.

It should be pointed out that the intrinsic vertical polarization of the laser beam is not known. The relative alignment between the intrinsic polarization vector and the wire-grid polarizer presumably affected the throughput of the system at some level, but this effect should not be important close the minimum in the plotted curve.

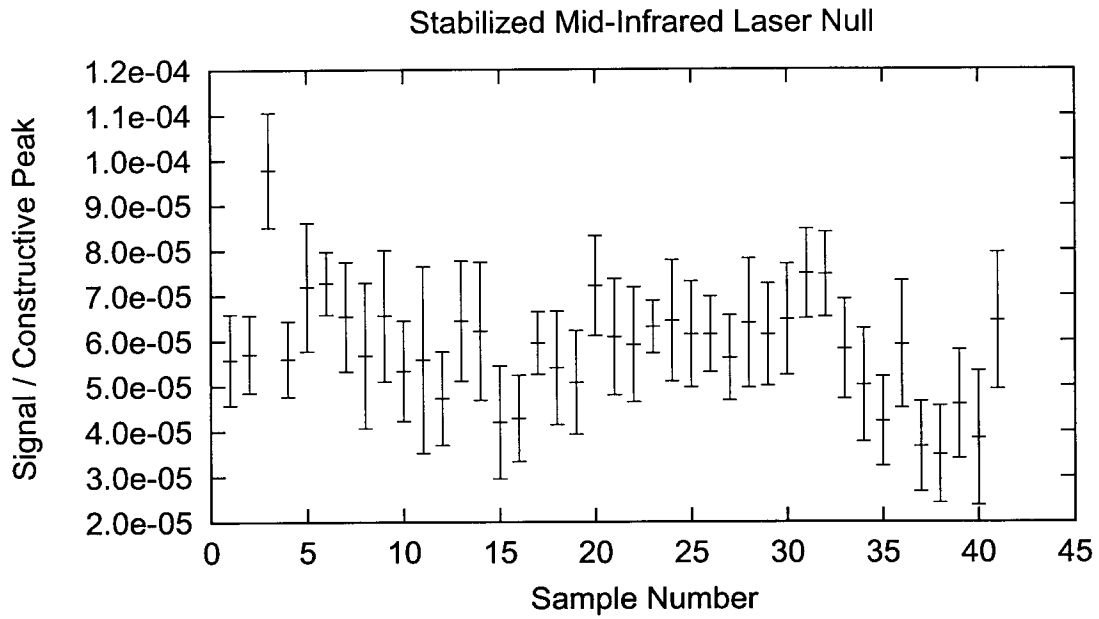


Figure 5. Stabilized null depth for a series of samples.

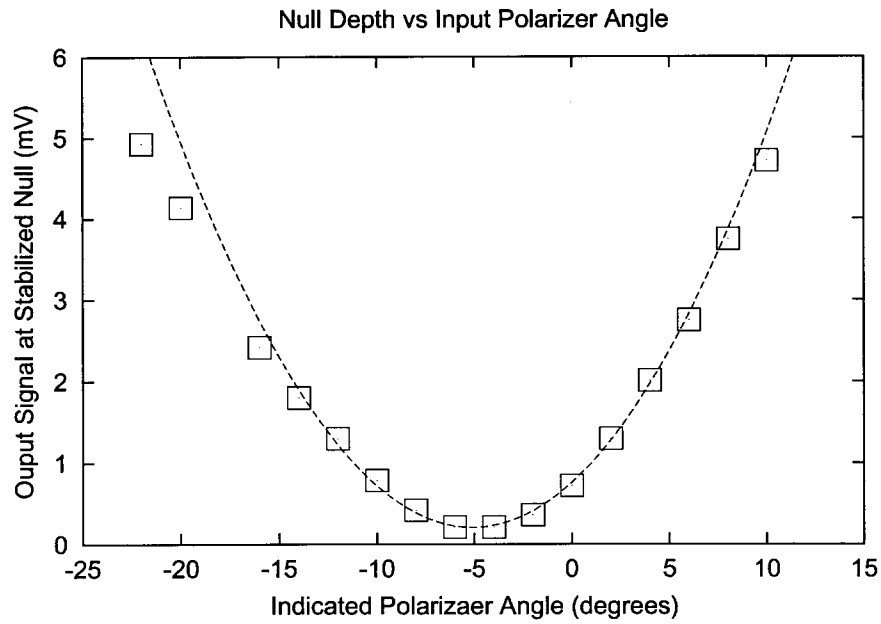


Figure 6. Signal measured at a stabilized null, as a function of polarizer position angle.

#### 5.4. Balancing the Fluxes in the Arms

An imbalance in the flux contributed by the two arms in the nuller leads to a leakage term which limits the depth of the null. The flux in the each arm could be measured easily by blocking the other and observing the detected signal. When the system was well aligned, these were typically different from each other by about 10%.

Two methods for equalizing the flux were tried. The first was to deliberately misalign the arm showing the larger throughput. This method had been used successfully for the visible-light tabletop nuller (Serabyn et al. 1999), but it never worked very well for the infrared nuller. We suspect that this is a result of the use of a pinhole rather than a single-mode fiber as a spatial filter, as the pinhole was not able to completely eliminate the ....?

The second flux-balancing method was to partially block the beam in the arm with the higher flux by inserting an object into the collimated space. Both irises and single-element "Venetian blinds" were used, with the latter giving more satisfactory results. This is probably due to the different ways the diffraction produced by these objects change the focussed image at the detector: the iris causes the Airy spot produced by a single arm to expand relative to that produced by the other, while the "Venetian blind," which consisted of a thin vertically-mounted strip of metal which could be rotated about its vertical axis to adjust its projected width, simply diffracted the excess light out of the beam while leaving the Airy spot essentially unchanged.

### 6. CONCLUSIONS

The experiments presented here have demonstrated that fringes with contrast in excess of  $10^4$  can be produced and stabilized at mid-infrared wavelengths. The best fringes were made with vertically-polarized, narrow-band light from a diode laser source. Both chromatic and polarization effects were significant when a less ideal light source was used.

To some extent the sensitivity to these adverse effects is inherent in the asymmetrical design of the rooftop beam combiner. The beam paths in the two arms must traverse several dielectric coatings, and in fact the number of such passages is larger by two in the arm containing the compensator plate. Further, the reflection at the beamsplitter in that arm occurs at an air/dielectric interface, while for the other arm it is at the interface between the beamsplitter and its substrate. It is therefore not surprising that the wavefronts contributed by the two arms have significantly different properties. This has led us to move on to a much more symmetrical beam-combiner design for further nulling work.

### ACKNOWLEDGMENTS

Funding was provided by NASA through the Keck Interferometer and Terrestrial Planet Finder projects. The research presented here was conducted at the Jet Propulsion Laboratory, California Institute of Technology, under contract with the National Aeronautics and Space Administration.

### REFERENCES

1. E. Serabyn, J.K. Wallace, G.J. Hardy, E.G.H. Schmidlin, & H. Nguyen, "Deep Nulling of Visible Laser Light", *Applied Optics*, 38, 7128-7132, 1999
2. E. Serabyn, "Nulling Interferometry: Symmetry Requirements and Experimental Results", in *Proc. SPIE 4006*, "Interferometry in Optical Astronomy," eds. P.J. Lena & A. Quirrenbach, 328-339, 2000